

# Synthesis and Vibrational Spectroscopic Investigation of Methyl L-Proline Hydrochloride: A Computational Insight

V. Balachandran<sup>1</sup>,  
M. Boobalan<sup>2,3</sup>,  
M. Amaladasan<sup>2</sup>,  
and S. Velmathi<sup>4</sup>

<sup>1</sup>P.G. & Research Department of Physics, Arignar Anna Government Arts College, Tiruchirappalli, India

<sup>2</sup>Department of Chemistry, St. Joseph's College, Tiruchirappalli, India

<sup>3</sup>Department of Chemistry, Roever Engineering College, Perambalur, India

<sup>4</sup>Department of Chemistry, National Institute of Technology, Tiruchirappalli, India

**ABSTRACT** In our present work, methyl L-proline hydrochloride has been synthesized from L-proline amino acid and characterized by Fourier transform infrared and Fourier transform Raman spectra via experimental and computational methods. Ab initio Hartree-Fock and density functional theory (B3LYP) calculations have been made for the structure, and atomic charge distributions were also predicted for the title compound by using the 6-311++G(d,p) basis set. Predicted vibrational frequencies have been assigned and compared with experimental Fourier transform infrared and Fourier transform Raman spectra. The thermodynamic properties such as heat capacity, enthalpy, entropy, and Gibbs energy have been calculated at different temperatures. The calculated highest occupied molecular orbital and lowest unoccupied molecular orbital energy show the charge transfer behavior within the molecule.

**KEYWORDS** density functional theory, Hartree-Fock, highest occupied molecular orbital, lowest unoccupied molecular orbital, methyl L-proline hydrochloride, synthesis, thermodynamic functions

## INTRODUCTION

L-Proline is an amino acid, which has one secondary amine and a carboxylic acid functional group with a chiral center. It is not an essential amino acid because the human body can synthesize it. L-Proline is one DNA-encoded amino acid out of 20 amino acids. It is a five-member hetero ring system having one nitrogen and four carbon annular atoms, and this contributes to it having a rigid ring structure, which leads to its special characteristic features such as the bending template effect in peptide chains. The synthetic products of L-proline derivatives show significant biological activity and organo catalytic behavior. Especially, they are used in enantio-selective aldol, Mannich, and Michael addition reactions and in the synthesis of certain macrocyclic molecular systems.<sup>[1–5]</sup>

L-Proline is the derivative of glutamine amino acid. It has a significant role in the human biological system. It contributes to the healthy functioning of the bone, muscles, skin, and immune system. A deficiency in this amino acid might lead an individual to have tears in tissues and very slow healing ability.

Received 27 December 2012;  
accepted 10 August 2013.

Address correspondence to M. Boobalan, Department of Chemistry, St. Joseph's College, Tiruchirappalli 620002, India.  
E-mail: Jerry.Fedrick@gmail.com  
Department of Chemistry, Roever Engineering College, Perambalur 621212, India

Color versions of one or more of the figures in the article can be found online at [www.tandfonline.com/isl](http://www.tandfonline.com/isl).

This paucity can be rectified by a healthy and balanced diet and supplements suggested by a physician.<sup>[6]</sup>

The various computational investigations have been made on several derivatives of L-proline and L-proline individual residue.<sup>[7]</sup> For instance, Wagner et al.<sup>[8]</sup> investigated the vibrational frequencies of the copper complex of L-proline. Sheena Mary et al.<sup>[9]</sup> reported the vibrational spectra such as Fourier transform infrared (FT-IR), Fourier transform Raman (FT-Raman), and surface-enhanced Raman spectral (SERS) studies of L-proline. Recently, vibrational spectra of L-proline and its hydrated complex have been reported based on density functional theory (DFT) and MP2 theories.<sup>[10]</sup> To the best of our knowledge, we can say that there is not any scientific communication on methyl L-prolinate hydrochloride under vibrational spectroscopic computation. The vibrational spectroscopic techniques such as FT-IR and FT-Raman are believed to be an effective experimental technique to understand the structural and vibrational behavior of the molecule. So the methyl L-prolinate hydrochloride has been critically examined based on these spectral techniques and special attention given to explain all the remarkable qualitative and quantitative differences in these spectra. The possible rotational isomers of methyl L-prolinate hydrochloride have been searched. There are eight different rotational isomers found for this title compound. The optimized geometry and vibrational wavenumber for a stable isomer of the title compound were calculated at Hartree-Fock (HF) and B3LYP levels of theory with the 6-311++G(d,p) basis set. The results of the theoretical and spectroscopic studies are reported herein. Detailed interpretations of the vibrational spectra of methyl L-prolinate hydrochloride have been made. The atomic charges of methyl L-prolinate hydrochloride were investigated using HF and B3LYP levels with the 6-311++G(d,p) basis set. The calculated highest occupied molecular orbital (HOMO) and lowest unoccupied molecular orbital (LUMO) energy give information on charge transfer behavior that takes place within the molecule. Various thermodynamic functions are also calculated by different temperatures.

## EXPERIMENTAL

The FT-IR spectra of methyl L-prolinate hydrochloride were recorded at room temperature in the

region 4000–400  $\text{cm}^{-1}$  using a Perkin-Elmer spectrum RX1 spectrophotometer using the KBr pellet technique. The signals were collected for 100 scans with a scan interval of 1  $\text{cm}^{-1}$  and at an optical resolution of 0.4  $\text{cm}^{-1}$ . The FT-Raman spectrum was also recorded in the region 3500–100  $\text{cm}^{-1}$  using a Bruker-FRA 106/IFS100 spectrometer. The spectrometer consists of a quartz beam splitter and a highly sensitive germanium diode detector cooled to the liquid nitrogen temperature. The sample was packed in a glass tube of about 5 mm diameter and excited in the 180° geometry with a 1064-nm laser line at 75 mW power from a diode-pumped air-cooled-cw Nd:YAG laser as excitation wavelength in the region of 3500–100  $\text{cm}^{-1}$ . The signals were collected for 300 scans at the interval of 1  $\text{cm}^{-1}$  and optical resolution of 0.1  $\text{cm}^{-1}$ .

## Synthesis

Optically active L-proline amino acid was purchased from LOBA Chemie and was commercial grade and used without further purification for the synthesis of methyl L-prolinate hydrochloride. About 1.0 g (6.0379 mmol) of L-proline was treated with methanol in the presence of 0.7183 g (6.0379 mmol) of  $\text{SOCl}_2$  to form this ester. It was synthetically an effective and well-known acid-catalyzed method for this esterification process.<sup>[11]</sup> Since the addition of  $\text{SOCl}_2$  was an exothermic reaction, the entire reaction system was maintained under ice bath for about 24 hr in a fume hood chamber. The completion of the reaction and purity of the product were checked during reasonable intervals using precoated Merck graded thin layer chromatographic (TLC) plates in the mixture of the hexane and ethyl acetate solvent system. Finally, the formed ester was separated using a Roto Vacuum Evaporator branded from Buche Labortechnik AG with appropriate temperature and pressure. The percentage of yield was >98%. The scheme of the reaction is shown in Fig. 1.

## Computational Methods

The molecular structure of methyl L-prolinate hydrochloride and the corresponding vibrational harmonic frequencies were calculated using HF and B3LYP theory combined with 6-311++G(d,p) basis set model chemistries. All these calculations



**FIGURE 1** Synthesis scheme of methyl L-prolinate hydrochloride.

were performed using the GAUSSIAN09W quantum chemistry program package<sup>[12]</sup> on a Pentium IV processor personal computer without constrained geometry for the stable isomer, but the rest of the other isomers were constrained. A close agreement between observed and calculated frequencies was achieved by means of the least square fit refinement algorithm. In our present scenario, the frequencies of the title molecule are scaled with four different scaling factors. In the HF level, the frequencies above  $1701\text{ cm}^{-1}$  are scaled with 0.9287, and other frequencies, which fall below  $1700\text{ cm}^{-1}$ , are scaled with 0.9116. In the case of B3LYP, the scaling factors of 0.9731 and 0.9561 are used in between the above said two different ranges of frequencies, respectively.

## RESULTS AND DISCUSSION

### Conformational Stability

An intensive study was carried out to identify the most stable isomer out of eight possible isomers of methyl L-prolinate hydrochloride. All the eight possible isomers come to survive because of free rotation of atoms in  $-\text{COOCH}_3$  group functionality. The pictorial representations of all eight isomers are shown in Fig. 2. The study on energy calculation is performed with the Gaussian09W program and the results are viewed in GaussView 5.0.8 GUI.<sup>[13]</sup> All the energies are tabulated in Table 1, and isomer "R5" is considered as the most stable isomer. Therefore, further in this article, we focus on this particular isomer and consider it the title molecule; also, all the computational investigations are executed based on this most stable isomer.

### Molecular Geometry

The optimized geometry and labeling of atoms in methyl L-prolinate hydrochloride are given in Fig. 3. In our present work, we performed full geometry

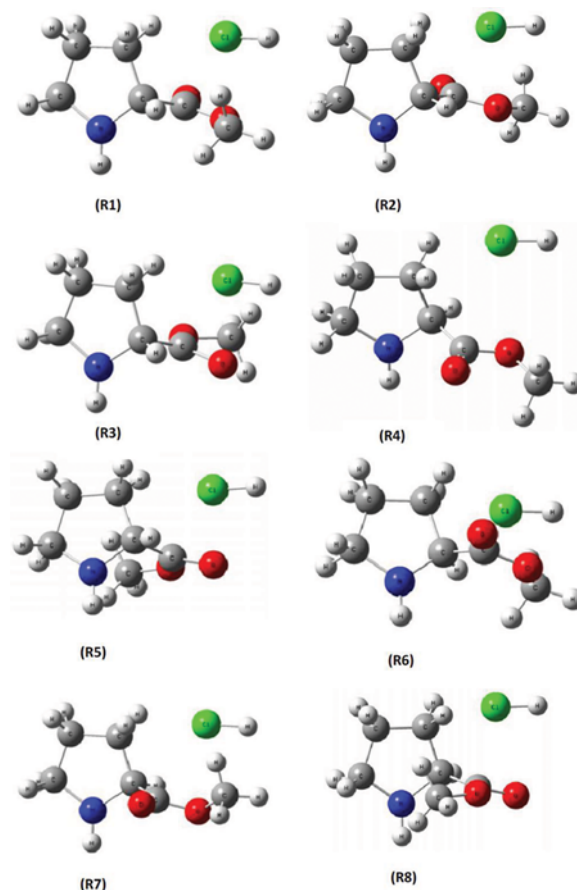


**FIGURE 2** Possible rotational isomer geometry of methyl L-prolinate hydrochloride.

optimization on the title molecule. The optimized structural parameters are calculated by ab initio and DFT methods listed in Table 2. After careful scrutiny, we came to know that the crystallographic data of methyl L-prolinate hydrochloride is not available in the literature. Therefore, the optimized structure can only be compared with the crystal structure of other similar systems such as L-proline and DL-proline.<sup>[14]</sup> The experimental geometric parameters are much closer to the results of the B3LYP method than the HF method. The optimized C(4)-C(5) bond length shows good consistency between HF, B3LYP, and experimental results. The experimental C(4)-C(5)

**TABLE 1** Calculated Energies and Energy Difference for Eight Rotational Isomers of Methyl L-Proline Hydrochloride by HF/6-311++G(d,p) and B3LYP/6-311++G(d,p) Methods

Isomers	HF/6-311++G(d,p)		B3LYP/6-311++G(d,p)	
	Energy (Hartree)	Relative energy <sup>a</sup> (Hartree)	Energy (Hartree)	Relative energy <sup>a</sup> (Hartree)
R1	-897.8723	0.0650	-901.3174	0.0568
R2	-897.8570	0.0803	-901.3049	0.0693
R3	-897.8050	0.1323	-901.2579	0.1163
R4	-897.8224	0.1149	-901.2740	0.1002
R5	-897.9373*	0.0000	-901.3742*	0.0000
R6	-897.8511	0.0862	-901.3027	0.0715
R7	-897.9267	0.0106	-901.3625	0.0117
R8	-897.8861	0.0512	-901.3294	0.0448

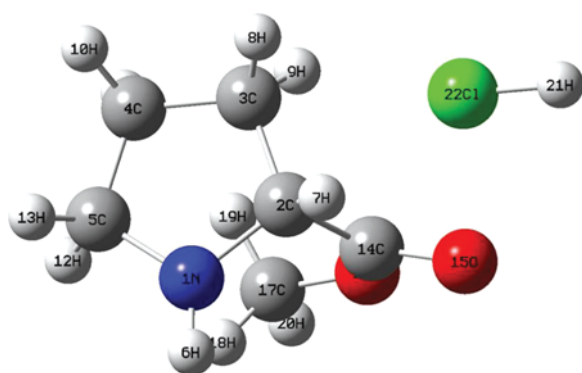
<sup>a</sup>Energies of the other three isomers relative to the most stable "R5" isomers.

\*Minimum energy geometry.

bond length is  $1.53 \text{ \AA}$ , which is identically produced by HF and B3LYP results. Nevertheless, the computed bond length in N(1)-C(5), N(1)-H(6), C(2)-C(3), C(3)-C(4), C(3)-H(8), C(3)-H(9), C(4)-H(10), C(4)-H(11), and C(5)-H(12) are varying by  $0.01 \text{ \AA}$  against the experimental bond length. The comparative and regressive correlation graphs are plotted between experimental and computed values of both bond length and bond angle. The graphical presentation is given in Figs. 4 and 5. The correlative regression value for bond length shows the existence of a higher degree of closeness between the computed and experimental results. However, the bond angle value is very poor due to the comparison between stereochemically different DL-proline molecular systems with the title molecule.

## Vibrational Assignment

The vibrational spectra of methyl L-proline hydrochloride have not been reported in detail in

**FIGURE 3** Optimized stable isomer geometry of methyl L-proline hydrochloride.

any literature. Therefore, we focused on this derivative of L-proline. The FT-IR and FT-Raman spectra of the title compound are compared with the theoretically calculated vibrational spectra by the HF and B3LYP methods with the 6-311++G(d,p) basis set and are shown in Figs. 6 and 7, respectively. The envisaged vibrational spectrum has no imaginary frequency, implying that the optimized geometry is located at the local minimum. Since the ab initio and DFT potentials steadily overrate the vibrational wavenumber, the divergence can be minimized by implementing an appropriate scaling procedure with a suitable numerical scaling factor. Theoretical and experimental frequencies are compared and tabulated in Table 3. All calculated spectra are in good accordance with experimental data. The calculated frequencies are slightly higher than experimental frequencies for the majority of the normal modes. Some factors might be responsible for discrepancies between the experimental and computed spectra of this title compound. One is probably the interaction with the surrounding molecules, and the other one is harmonic oscillator approximation in theoretical calculations; it should be noted that theoretical calculations neglect the anharmonic effects. Besides, the errors in calculated frequencies result from the inadequate basis set or from the lack of the electron correlation. A linear relation was found between experimental and theoretical frequencies that are plotted in Fig. 8.

## N-H Vibrations

The title molecule methyl L-proline hydrochloride has a secondary amine group in which the

**TABLE 2** Computed Optimized Geometrical Parameters of Methyl L-Proline Hydrochloride by HF/6-311++G(d,p) and B3LYP/6-311++G(d,p) Methods

Bond length (Å)				Bond angle (degrees)			
Parameters	HF/6-311++ G(d,p)	B3LYP/6-311++ G(d,p)	Exp	Parameters	HF/6-311++ G(d,p)	B3LYP/6-311++ G(d,p)	Exp
N1-C2	1.45	1.47	1.47	C2-N1-C5	106.60	106.44	110.1
N1-C5	1.46	1.47	1.46	C2-N1-H6	111.89	111.64	115.5
N1-H6	1.00	1.01	1.00	C5-N1-H6	112.51	112.68	116.0
C2-C3	1.55	1.56	1.56	N1-C2-C3	104.75	104.54	104.2
C2-H7	1.08	1.10	1.08	N1-C2-H7	111.91	112.01	111.7
C2-C14	1.53	1.53		N1-C2-C14	114.56	114.12	113.0
C3-C4	1.54	1.55	1.54	C3-C2-H7	108.71	108.55	111.8
C3-H8	1.08	1.09	1.08	C3-C2-C14	113.59	114.37	108.7
C3-H9	1.08	1.09	1.08	H7-C2-C14	103.39	103.35	107.5
C4-C5	1.53	1.53	1.53	C2-C3-C4	104.61	104.85	104.3
C4-H10	1.08	1.09	1.08	C2-C3-H8	109.30	109.07	109.0
C4-H11	1.08	1.09	1.08	C2-C3-H9	112.59	112.64	111.4
C5-H12	1.08	1.09	1.08	C4-C3-H8	111.80	111.77	109.2
C5-H13	1.09	1.10	1.08	C4-C3-H9	111.88	111.86	113.1
C14-O15	1.19	1.22	1.20	H8-C3-H9	106.74	106.72	109.0
C14-O16	1.32	1.34		C3-C4-C5	103.91	103.97	101.4
C14-Cl22	4.18	3.99		C3-C4-H10	112.43	112.35	112.9
O16-C17	1.42	1.44		C3-C4-H11	110.66	110.63	109.8
C17-H18	1.08	1.09		C5-C4-H10	112.49	112.41	113.0
C17-H19	1.08	1.09		C5-C4-H11	109.73	109.78	109.2
C17-H20	1.08	1.09		H10-C4-H11	107.63	107.71	109.8
H21-Cl22	1.28	1.31		N1-C5-C4	102.66	102.43	101.0
				N1-C5-H12	110.72	110.50	110.4
				N1-C5-H13	112.09	112.46	112.5
				C4-C5-H12	113.16	113.23	112.9
				C4-C5-H13	110.25	110.24	110.4
				H12-C5-H13	107.97	108.01	109.6
				C2-C14-O15	119.11	119.33	
				C2-C14-O16	122.55	122.78	
				C2-C14-Cl22	154.15	157.90	
				O15-C14-O16	118.32	117.88	
				O15-C14-Cl22	35.06	39.00	
				O16-C14-Cl22	83.26	79.03	
				C14-O16-C17	127.26	125.11	
				O16-C17-H18	110.85	110.87	
				O16-C17-H19	111.80	109.97	
				O16-C17-H20	104.64	104.64	
				H18-C17-H19	109.60	110.76	
				H18-C17-H20	110.49	111.26	
				H19-C17-H20	109.37	109.17	
				C14-Cl22-H21	10.18	11.76	

nitrogen acts as an annular atom in the five-member ring system. In general, the N-H stretching vibration in the FT-IR spectrum is expected in the range near 3400–3500 cm<sup>-1</sup>.<sup>[10]</sup> The experimentally observed spectrum shows 3473 cm<sup>-1</sup>. This observation agrees well with the theoretically calculated value. The

N-H in-plane bending vibrations usually occur in the region of 1650–1580 cm<sup>-1</sup>. In the present title molecule, the one medium FT Raman band is observed at 1413 cm<sup>-1</sup>.

On considering the N-H out-of-plane bending vibrations, one can expect the frequency around

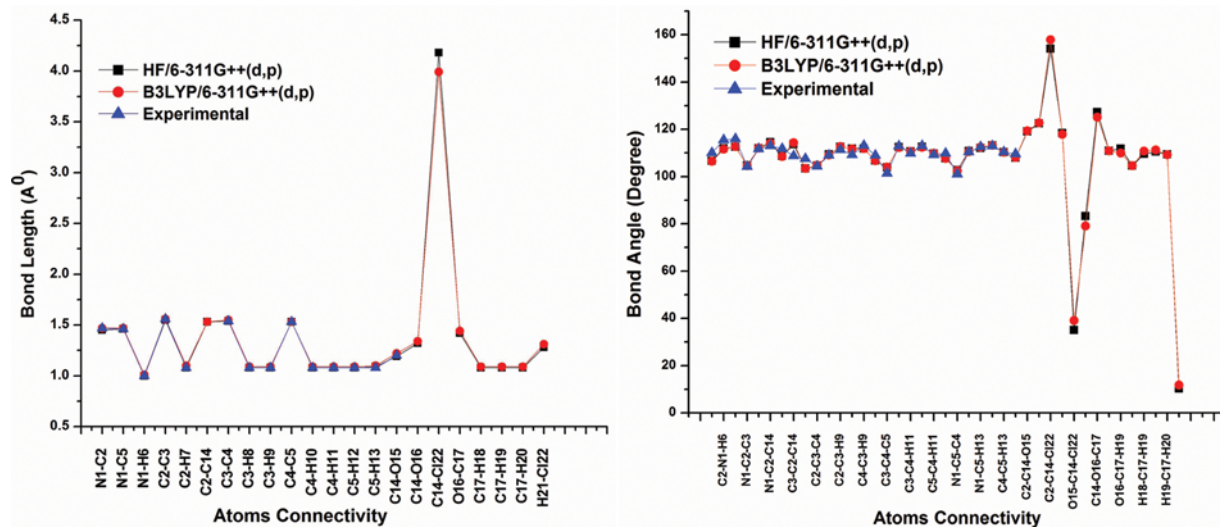


FIGURE 4 Comparison between experimental and computed bond length and bond angle in the HF and B3LYP approaches.

$895\text{ cm}^{-1}$ .<sup>[15]</sup> It has good agreement with both the observed and theoretical FT-IR and Raman values. The observed frequencies are  $838\text{ cm}^{-1}$  in Raman and the theoretical frequencies are  $854$  and  $840\text{ cm}^{-1}$  in HF and B3LYP, respectively. From the observed N-H vibrations, both stretching and bending vibrations shows good agreement with expectations, except with N-H in-plane bending, due to the impact of other substitutions.

## CH<sub>2</sub> Vibrations

Methylene is involved in various modes of vibrations such as asymmetry, symmetry stretching, scissoring, wagging, twisting, and rocking in their

respective regions of frequency. An isolated C-H bond has only one stretching frequency, but the stretching vibrations of the C-H bond in the CH<sub>2</sub> group combine together to produce two coupled vibrations of different frequencies described as asymmetric and symmetric frequencies, with the asymmetric often being the higher frequency. It is noted while the bonds are very close to each other in the CH<sub>2</sub> system and have a similar frequency, they can easily undergo vibrational coupling, or the fundamental vibration may be coupled with an overtone of some other vibration to show Fermi resonance behavior.

The vibrations of the CH<sub>2</sub> group, the asymmetric stretch  $\nu_{\text{as}}\text{CH}_2$ , the symmetric stretch  $\nu_{\text{s}}\text{CH}_2$ , the scissoring vibrations of the  $\delta\text{CH}_2$ , and the wagging

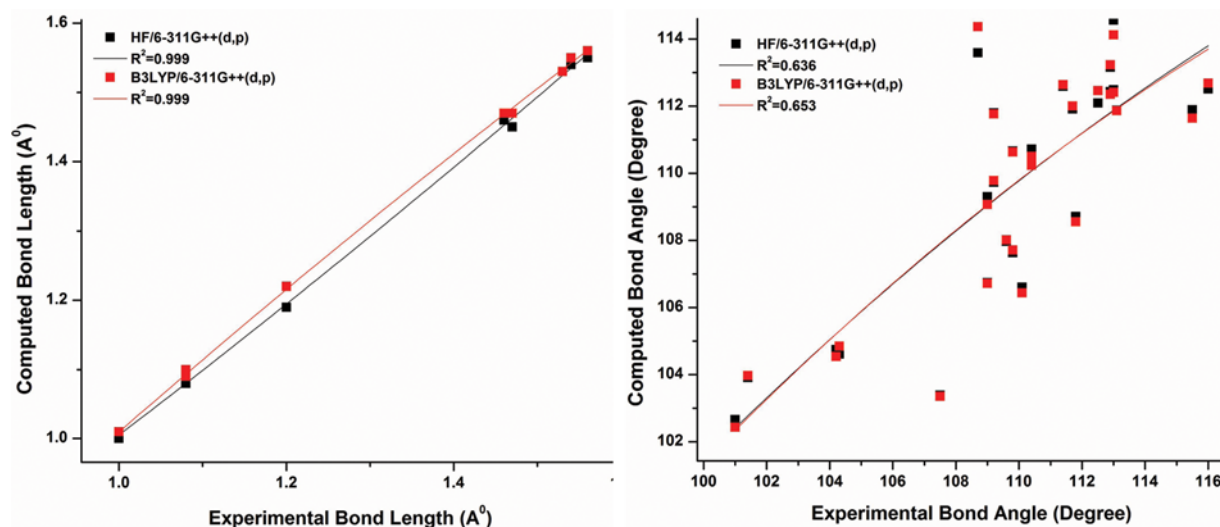
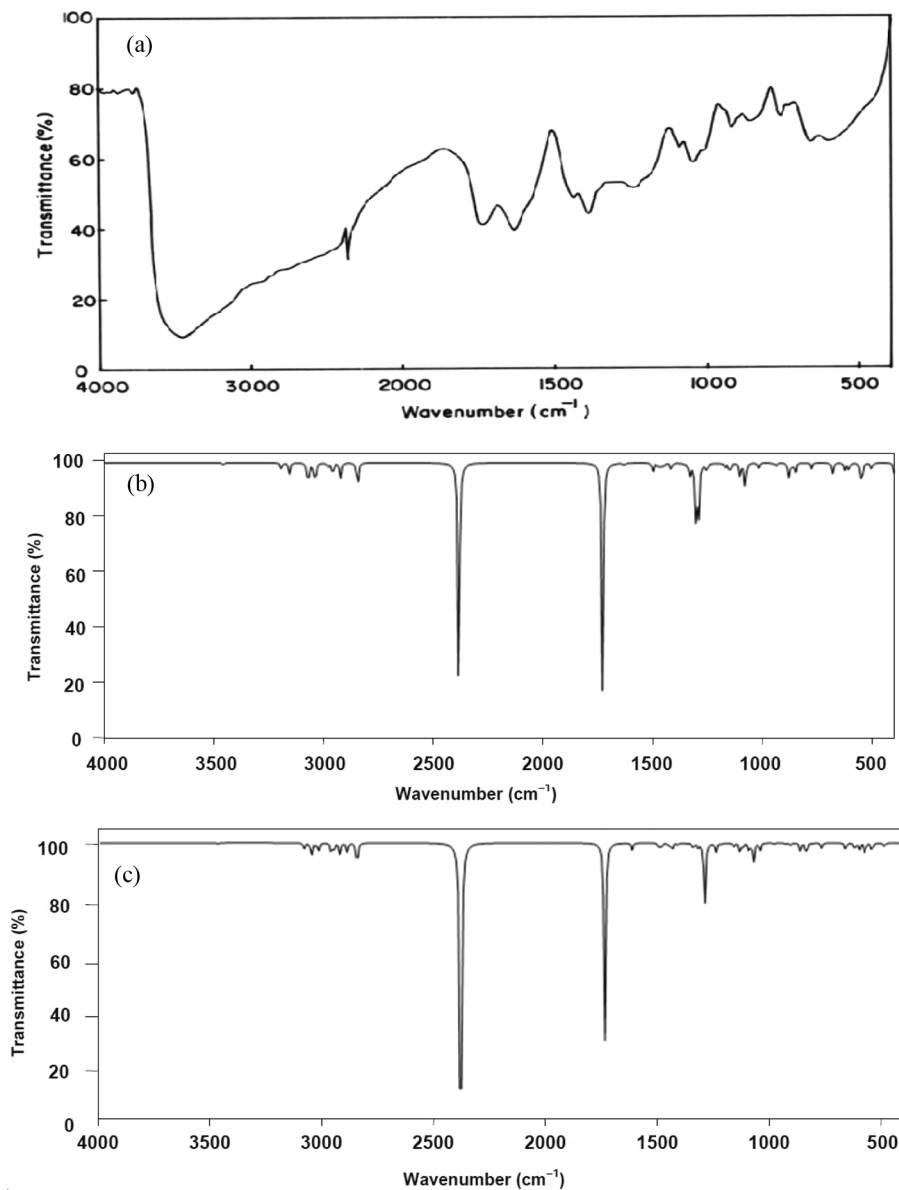


FIGURE 5 Correlation plot between experimental and computed bond length and bond angle in the HF and B3LYP approaches.



**FIGURE 6** FT-IR spectra of methyl L-prolinate hydrochloride: (a) observed, (b) calculated by HF/6-311+G(d,p) and scaled, and (c) calculated by B3LYP/6-311+G(d,p) and scaled.

vibration of the  $\omega\text{CH}_2$ , appear in the regions  $3000 \pm 50$ ,  $2965 \pm 30$ ,  $1455 \pm 55$ , and  $1350 \pm 85 \text{ cm}^{-1}$ , respectively.<sup>[16,17]</sup> Methylene asymmetric and symmetric stretching bands of the pyrrolidine are usually observed near  $2953$  and  $2868 \text{ cm}^{-1}$ , respectively.<sup>[18]</sup> The HF and B3LYP calculations give three bands for the asymmetric and symmetric stretching corresponding to different methylene groups, C(1)-H(2)-H(3), C(4)-H(5)-H(6), and C(7)-H(8)-H(9). Electronic effects including back donation, mainly caused by the presence of the nitrogen atom adjacent to the methylene groups, can shift the position and alter the intensity of CH stretching and bending modes.

The lowering of wavenumbers and the increasing intensity of CH stretching modes of the  $\text{CH}_2$  of the ring point to the influence of back donation in the ring owing to the presence of the nitrogen atom. For a molecule containing a methylene group, the electronic charge is back donated from the lone pair of nitrogen to the  $\sigma^*$  orbital of the CH bonds, causing a weakening of the CH bonds. This is followed by the increase in C-H force constants and can result in the enhancement of IR band intensity of C-H stretching modes.<sup>[19,20]</sup> The asymmetric  $\text{CH}_2$  stretching bands are observed at  $3048$ ,  $3036$ , and  $3024 \text{ cm}^{-1}$  in the FT-Raman spectrum. The calculated values are



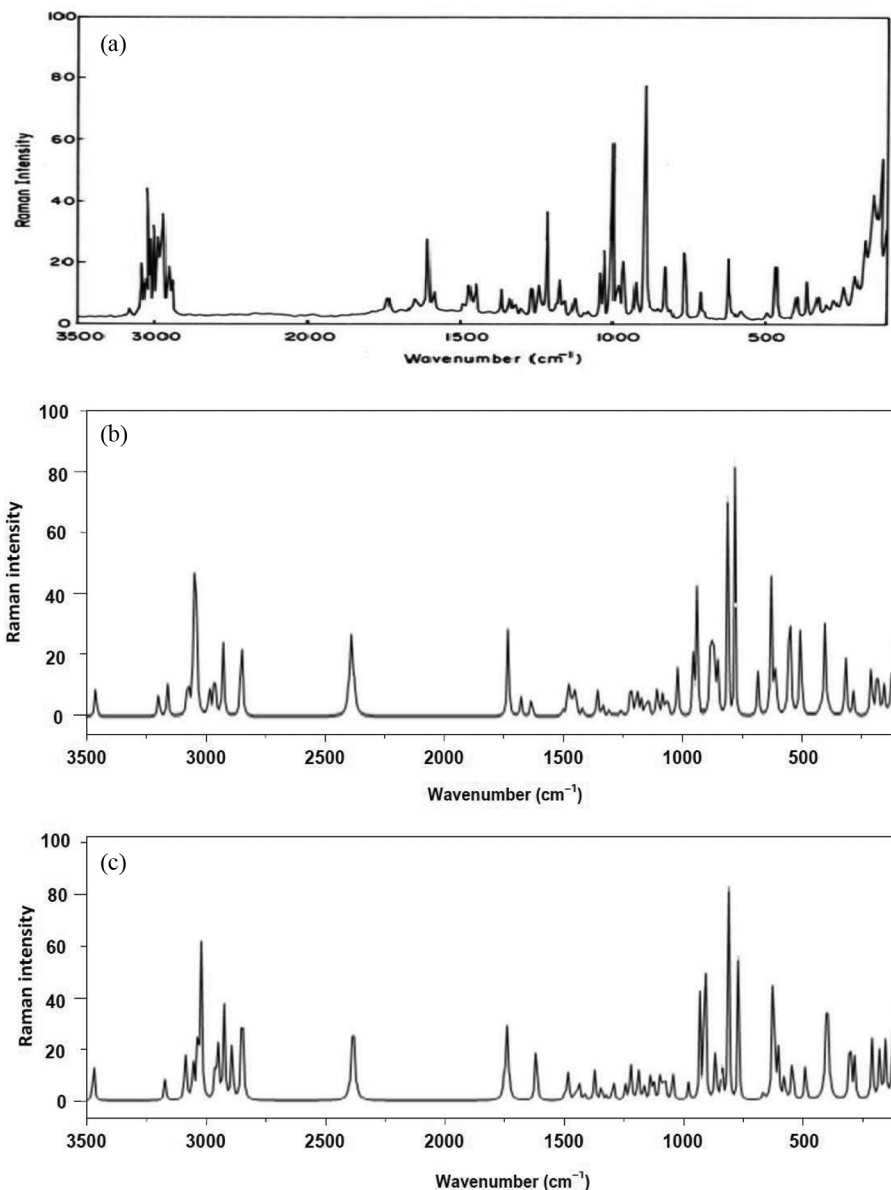


**FIGURE 7** FT-Raman spectra of methyl L-prolinate hydrochloride: (a) observed, (b) calculated by HF/6-311+G(d,p) and scaled, and (c) calculated by B3LY/6-311+G(d,p) and scaled.

3072, 3048, and 3040  $\text{cm}^{-1}$  and 3054, 3035, and 3021  $\text{cm}^{-1}$  by HF and B3LYP levels, respectively. The symmetrical  $\text{CH}_2$  stretching bands are observed at 2975, 2950, and 2923  $\text{cm}^{-1}$  in the Raman spectra.

The bending vibrations of the C-H bonds in the methylene group are identified in their respective positions. The scissoring mode of the  $\text{CH}_2$  group gives rise to a characteristic band observed near 1465  $\text{cm}^{-1}$  in the literature.<sup>[21]</sup> The twisting and rocking vibrations of the  $\text{CH}_2$  group appear in the regions  $1290 \pm 45$  and  $890 \pm 55$   $\text{cm}^{-1}$ , respectively.<sup>[15]</sup> The twisting and rocking modes are also identified. For proline oligomers and poly-L-proline,<sup>[22]</sup> the  $\text{CH}_2$

deformation bands are reported at 1446, 1261, and 1237 ( $\delta\text{CH}_2$ ); 1198, 1187, and 1172 ( $\tau/\omega\text{CH}_2$ ); and 781 and 662  $\text{cm}^{-1}$  ( $\rho\text{CH}_2$ ). For the title molecule, the bands are observed at 1494, 1475, and 1450  $\text{cm}^{-1}$  in the Raman spectrum, and the calculated frequencies 1502, 1479, and 1464  $\text{cm}^{-1}$  and 1496, 1483, and 1455  $\text{cm}^{-1}$  by HF and B3LYP, respectively, are ascribed to the  $\text{CH}_2$  scissoring modes. The  $\text{CH}_2$  wagging modes are observed at 1325, 1275, and 1250  $\text{cm}^{-1}$  in the Raman spectrum, and the values 1308, 1295, and 1257  $\text{cm}^{-1}$  and 1324, 1302, and 1245  $\text{cm}^{-1}$  are theoretically calculated by HF/6-311++G(d,p) and B3LYP/6-311++G(d,p), respectively. For the title molecule,



**TABLE 3** Calculated Vibrational Frequencies ( $\text{cm}^{-1}$ ) Assignment of Methyl L-Proline Hydrochloride Based on HF/6-311++G(d,p) and B3LYP/6-311++G(d,p) Methods

No	Observed frequencies		Calculated frequencies				Assignment
	IR	Raman	HF/6-311++G(d,p)		B3LYP/6-311++G(d,p)		
			Unscaled	Scaled	Unscaled	Scaled	
01.	3473vs		3770	3458	3537	3470	$\nu$ NH
02.		3179m	3322	3194	3167	3171	$\nu_{\text{asym}}$ CH <sub>3</sub>
03.		3107s	3303	3157	3132	3086	$\nu_{\text{asym}}$ CH <sub>3</sub>
04.		3048m	3255	3072	3114	3054	$\nu_{\text{asym}}$ CH <sub>2</sub>
05.		3036s	3233	3048	3096	3035	$\nu_{\text{asym}}$ CH <sub>2</sub>
06.		3024m	3227	3040	3077	3021	$\nu_{\text{asym}}$ CH <sub>2</sub>
07.		2975m	3225	2982	3072	2961	$\nu_{\text{sym}}$ CH <sub>2</sub>
08.		2950m	3212	2960	3055	2949	$\nu_{\text{sym}}$ CH <sub>2</sub>
09.		2923m	3194	2925	3050	2924	$\nu_{\text{sym}}$ CH <sub>3</sub>
10.		2900m	3194	2924	3015	2891	$\nu$ CH
11.			3110	2847	2950	2848	$\nu_{\text{sym}}$ CH <sub>2</sub>
12.	2378s		2579	2386	2573	2384	$\nu$ HCl
13.	1737s	1744w	1940	1731	1739	1741	$\nu$ CO
14.		1636s	1655	1677	1630	1614	$\delta$ CH <sub>3</sub>
15.		1619w	1640	1633	1618	1620	$\delta$ CH <sub>3</sub>
16.		1494w	1527	1502	1512	1496	$\rho$ CH <sub>2</sub>
17.		1475m	1513	1479	1499	1483	$\rho$ CH <sub>2</sub>
18.		1465m	1508	1464	1493	1455	$\rho$ CH <sub>2</sub>
19.	1440m		1488	1449	1475	1439	$\rho$ CH <sub>3</sub>
20.		1413m	1465	1418	1443	1415	$\delta$ NH
21.	1387m	1375m	1520	1357	1388	1373	$\delta$ CH
22.		1344m	1495	1334	1362	1345	$\nu$ CC
23.		1325w	1465	1308	1338	1324	$\omega$ CH <sub>2</sub>
24.		1275s	1451	1295	1316	1302	$\omega$ CH <sub>2</sub>
25.			1434	1280	1308	1294	$\gamma$ CO
26.	1247m	1250m	1431	1257	1299	1245	$\omega$ CH <sub>2</sub>
27.		1225w	1363	1216	1255	1222	tCH <sub>2</sub>
28.		1188m	1334	1191	1219	1190	tCH <sub>2</sub>
29.		1165w	1314	1173	1205	1166	tCH <sub>2</sub>
30.		1131w	1291	1152	1178	1138	$\delta$ CH <sub>3</sub> rock
31.	1126m		1280	1142	1171	1125	$\gamma$ CH <sub>3</sub> rock
32.		1100m	1239	1106	1110	1098	$\nu$ CN
33.		1088m	1212	1082	1099	1087	$\nu$ CO
34.	1073m		1192	1064	1088	1077	$\nu$ CC
35.		1050vs	1144	1021	1057	1046	$\nu$ CC
36.		988m	1071	956	990	980	$\nu$ CN
37.	932w	925m	1044	940	962	932	$\nu$ CC
38.		900vs	990	884	921	911	$\delta$ Ring
39.	870w	868m	971	872	906	867	$\delta$ CO
40.	871w	838m	957	854	879	840	$\gamma$ NH
41.		813w	908	810	822	812	$\delta$ CH <sub>2</sub> rock
42.	775m		821	780	750	771	$\delta$ CO
43.	669m	675m	808	684	697	666	$\delta$ CO
44.		625w	704	628	649	625	$\delta$ Ring
45.	608w		684	610	635	605	$\delta$ CC
46.		580w	623	556	583	578	$\delta$ Ring
47.		544m	595	551	556	545	$\gamma$ HCl
48.		494m	532	506	500	490	$\delta$ HCl

(Continued)

**TABLE 3** Continued

No	Observed frequencies		Calculated frequencies				Assignment
	IR	Raman	HF/6-311++G(d,p)		B3LYP/6-311++G(d,p)		
			Unscaled	Scaled	Unscaled	Scaled	
49.		400 m	453	404	438	400	$\gamma$ CO
50.		306vw	355	317	333	304	$\gamma$ CO
51.		281vw	294	284	287	284	$\gamma$ CC
52.		213w	235	210	228	212	$\delta$ CH <sub>2</sub> rock
53.		181 m	206	184	201	180	$\delta$ CH <sub>2</sub> rock
54.		156 m	176	157	164	156	tCH <sub>3</sub> twist
55.		120 s	127	122	123	122	$\gamma$ CO
56.			98	87	112	88	$\nu$ O-HCl
57.			85	76	81	80	$\delta$ O-HCl
58.			69	62	70	60	$\gamma$ Ring
59.			22	20	34	21	$\gamma$ HCl
60.			18	16	20	16	$\gamma$ Ring

vs, very strong; s, strong; m, medium; w, weak; vw, very weak;  $\nu$ , stretching;  $\delta$ , in-plane bending;  $\gamma$ , out-of-plane bending;  $\sigma$ , scissoring;  $\omega$ , wagging; t, twisting.

the bands at 1225, 1188, and 1165 cm<sup>-1</sup> in the Raman spectrum and the calculated values 1222, 1190, and 1166 cm<sup>-1</sup> are assigned to the CH<sub>2</sub> twisting modes, whereas the bands at 813, 210, and 184 cm<sup>-1</sup> (HF) and 812, 212, and 180 cm<sup>-1</sup> (B3LYP) are assigned to the CH<sub>2</sub> modes.

### CH<sub>3</sub> Group Vibrations

The title compound methyl L-prolinate hydrochloride under consideration holds one CH<sub>3</sub> group. For the assignments of CH<sub>3</sub> group frequencies, one can expect the following fundamental modes that are associated to each CH<sub>3</sub> group, namely, the

symmetrical stretching in CH<sub>3</sub> (CH<sub>3</sub> symmetric stretch) and asymmetrical stretching (CH<sub>3</sub> asymmetric stretch); in-plane stretching modes (i.e., in-plane hydrogen stretching mode); the symmetrical (CH<sub>3</sub> symmetric deformation) and asymmetrical (CH<sub>3</sub> asymmetric deformation) deformation modes; and the in-plane rocking (CH<sub>3</sub> ipr), out-of-plane rocking (CH<sub>3</sub> opr), and twisting (tCH<sub>3</sub>) modes. In general, the methyl hydrogen atoms in the methyl group are subjected to back-donation, which causes the decrease of stretching wavenumbers and infrared intensities, as reported in the literature.<sup>[23]</sup> The computed values of two asymmetrical stretching vibrations of CH<sub>3</sub> originate at 3194 and 3157 cm<sup>-1</sup> in the HF and 3171

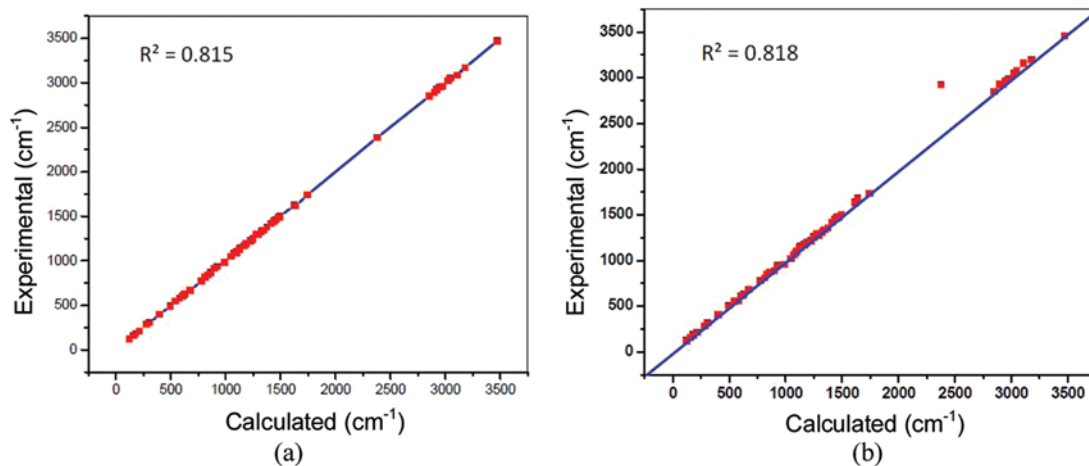


**FIGURE 8** Graphic correlation between the experimental and the theoretical frequencies obtained at the (a) HF/HF/6-311++G(d,p) level and (b) B3LYP/6-311++G(d,p) level.

and  $3086\text{ cm}^{-1}$  in the B3LYP methods, while experimental values are reported at  $3179$  and  $3107\text{ cm}^{-1}$  in the FT Raman spectrum. The theoretical  $\text{CH}_3$  symmetrical stretching frequency is found at  $2925$  and  $2924\text{ cm}^{-1}$  in the HF and B3LYP methods, while the experimental value is at  $2923\text{ cm}^{-1}$ . The calculated symmetric bending vibration using HF and B3LYP methods are  $1449$  and  $1439\text{ cm}^{-1}$ . But the experimental value contributes at  $1440\text{ cm}^{-1}$  in FT-IR. On considering the other vibrational modes of the  $\text{CH}_3$  group, in-plane rocking and out-of-plane rocking are observed at  $1152$  and  $1142\text{ cm}^{-1}$  in the HF and  $1138$  and  $1125\text{ cm}^{-1}$  in the B3LYP method, but the experimental value of in-plane rocking in FT-Raman is  $1131\text{ cm}^{-1}$ , and that of out-of-plane rocking is  $1126\text{ cm}^{-1}$  in FT-IR. Finally,  $\text{CH}_3$  twisting frequency is calculated and found as very lower frequency, that is,  $157$  and  $156\text{ cm}^{-1}$  in the above said methods; obviously, the experimental value is  $156\text{ cm}^{-1}$  under FT-Raman spectral data.

## C=O Vibrations

The stretching frequency of C=O and C-O provides effective information on structural elucidation of any esters. The C=O stretching vibration of saturated ester falls on  $1730$ – $1680\text{ cm}^{-1}$ . In general, three factors have the foremost impact in determining the frequency of the carbonyl group: inductive, resonance effects, and hydrogen bonding. Since there is no aromatic ring or hyperconjugative system, the frequency is not influenced by them. In addition, it is witnessed in our present study that the C=O stretching vibration is assigned to  $1744\text{ cm}^{-1}$  in FT-Raman and  $1737\text{ cm}^{-1}$  in FT-IR. The theoretical investigation at B3LYP/6-311++G\*\* shows significant agreement with real assignments. It lays on  $1741\text{ cm}^{-1}$ . Nevertheless, another theoretical platform does not show considerable accordance with the observed vibration whose value is  $1731\text{ cm}^{-1}$ . The C=O in-plane bending vibration is found at  $870\text{ cm}^{-1}$  in FT-IR and  $868\text{ cm}^{-1}$  in FT-Raman spectra, and the values  $867$  and  $872\text{ cm}^{-1}$  are calculated by the B3LYP and HF methods, respectively, under theoretical consideration. Another fashion of C=O out-of-plane bending vibration is expected at  $540 \pm 80$  frequency, but the observed value is  $400\text{ cm}^{-1}$  in FT-Raman and the computed value lay on  $404$  and  $400\text{ cm}^{-1}$  by HF and B3LYP consideration, respectively.

## Ring Vibrations

L-Proline is a five-membered nonaromatic N-heterocyclic chiral amino acid whose ring has maximum similarity with the pyrrolidine ring while excluding the carboxylic acid group. By comparing the frequency behavior of pyrrolidine annular atoms that form bonds in the ring such as C-C, C-N, we can easily afford to interpret the ring vibrations of the target molecule due to structural similarity. In general, the stretching vibrations of pyrrolidine ring regions are from  $1100$  to  $800\text{ cm}^{-1}$ . It is acknowledged with observed Raman values such as  $1100$ ,  $988\text{ cm}^{-1}$  corresponding to C-N vibration and according to the same, C-C vibration existence occurs at  $1050$ ,  $925\text{ cm}^{-1}$  equally  $932\text{ cm}^{-1}$  in FT-IR, finally at  $900\text{ cm}^{-1}$  in FT-Raman on the title molecule. The computed values on C-C, C-N vibrations have a noteworthy degree of closeness with the values of the B3LYP/6-311++G\*\* basis sets than those of the HF approach. This theoretical pattern is similar to ring in-plane-bending too. The entire ring in-plane bending is observed at  $625\text{ cm}^{-1}$  and  $608\text{ cm}^{-1}$  in FT-Raman and FT-IR, respectively.

## Mulliken Population Analysis: Mulliken Atomic Charges

Mulliken atomic charge calculation<sup>[24]</sup> has an important role in the application of quantum chemical calculation to the molecular system. Atomic charges of the skeleton atom for the title compound calculated at the HF/6-311++G(d,p) and B3LYP/6-311++G(d,p) model chemistries are presented in Table 4, because atomic charges affect dipole moment, polarizability, electronic structure, and more properties of molecular systems.

For the title compound the Mulliken atomic charges of H6 and H7 atoms occupy the higher positive value and become highly acidic. The corresponding Mulliken atomic charges of H6 and H7 are  $0.2651e$  and  $0.2625e$ , respectively, in B3LYP. The C3 and C17 atoms have a high negative value. The N1, O15, and O16 atoms have negative charges, whereas all hydrogen atoms have positive charges. The result suggests that the atoms N1, O15, and O16 are electron acceptors, which indicates that the charge shifts from H6 to N1, C17 to O16, and C14 to O15.

**TABLE 4** Mulliken Atomic Charges of Methyl L-Proline Hydrochloride Based on HF/6-311++G(d,p) and B3LYP/6-311++G(d,p) Methods

Atom	HF	B3LYP	Atom	HF	B3LYP
N1	-0.2508	-0.2157	H12	0.1581	0.1676
C2	-0.2394	-0.0205	H13	0.1440	0.1530
C3	-0.4698	-0.3359	C14	-0.0232	-0.0367
C4	-0.3136	-0.3167	O15	-0.3297	-0.2494
C5	-0.3006	-0.3432	O16	-0.2532	-0.1547
H6	0.2813	0.2651	C17	-0.3271	-0.3801
H7	0.2683	0.2625	H18	0.0180	0.2264
H8	0.1669	0.1647	H19	0.1522	0.1575
H9	0.1768	0.1572	H20	0.1772	0.1871
H10	0.1661	0.1735	H21	0.2779	0.2471
H11	0.1452	0.1466	Cl22	-0.2658	-0.2555

## HOMO–LUMO Energy Gap

In general, a molecule can be characterized by a highest occupied molecular orbital–lowest unoccupied molecular orbital (HOMO–LUMO) separation, which is the result of a significant degree of charge transfer from the end–capping electron–donor to the efficient electron acceptor group. This energy gap offers extensive information on the wavelength that a molecule can observe. The magnitude of energy gap is largely influenced by nature of conjugation.<sup>[25]</sup> A less conjugated system has a higher HOMO and LUMO gap. Therefore, a shorter wavelength is required for electronic excitation. With respect to methyl L-proline hydrochloride, the HOMO–LUMO energy gap value was found as 4.1646 eV in B3LYP/6-311++G(d,p) model chemistry. Since our target molecule does not have any pi conjugation, the energy gap was found to be high. Here, the charge transfer occurs from the five-membered heterocyclic ring residue system to the electron-withdrawing methyl ester fragment, under a shorter wavelength of light. The pictorial representation of HOMO and LUMO is given in Fig. 9.

## Thermodynamic Function Analysis

On the basis of B3LYP/6-311++G(d,p) vibrational analyses and statistical thermodynamics, the standard thermodynamic functions heat capacity ( $C_{p,m}^0$ ), entropy ( $H_m^0$ ), Gibbs energy ( $G_m^0$ ), and enthalpy ( $S_m^0$ ) of the title compound were obtained and are listed in Table 5. As shown in Table 5, all the values of  $C_{p,m}^0$ ,  $H_m^0$ , and  $S_m^0$  increase in temperature from 100.0 to 700 K, which was attributed to the

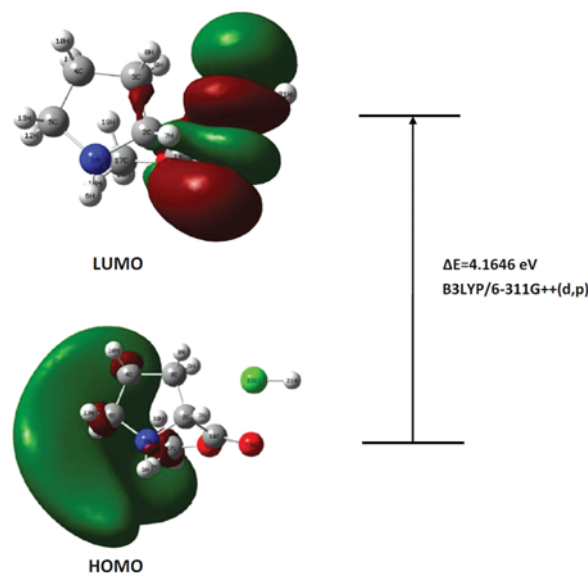
enhancement of the molecular vibration as the temperature increases.<sup>[26]</sup> The correlation equations between these thermodynamic properties and temperatures for the title compound are listed below. The correlations between these thermodynamic properties and temperatures  $T$  are shown in Fig. 10.

$$C_{p,m}^0 = 10.21 + 0.122T - 3.0 * 10^{-5}T^2 (R^2 = 0.998)$$

$$H_m^0 = 0.517 + 0.157T - 5.0 * 10^{-5}T^2 (R^2 = 0.999)$$

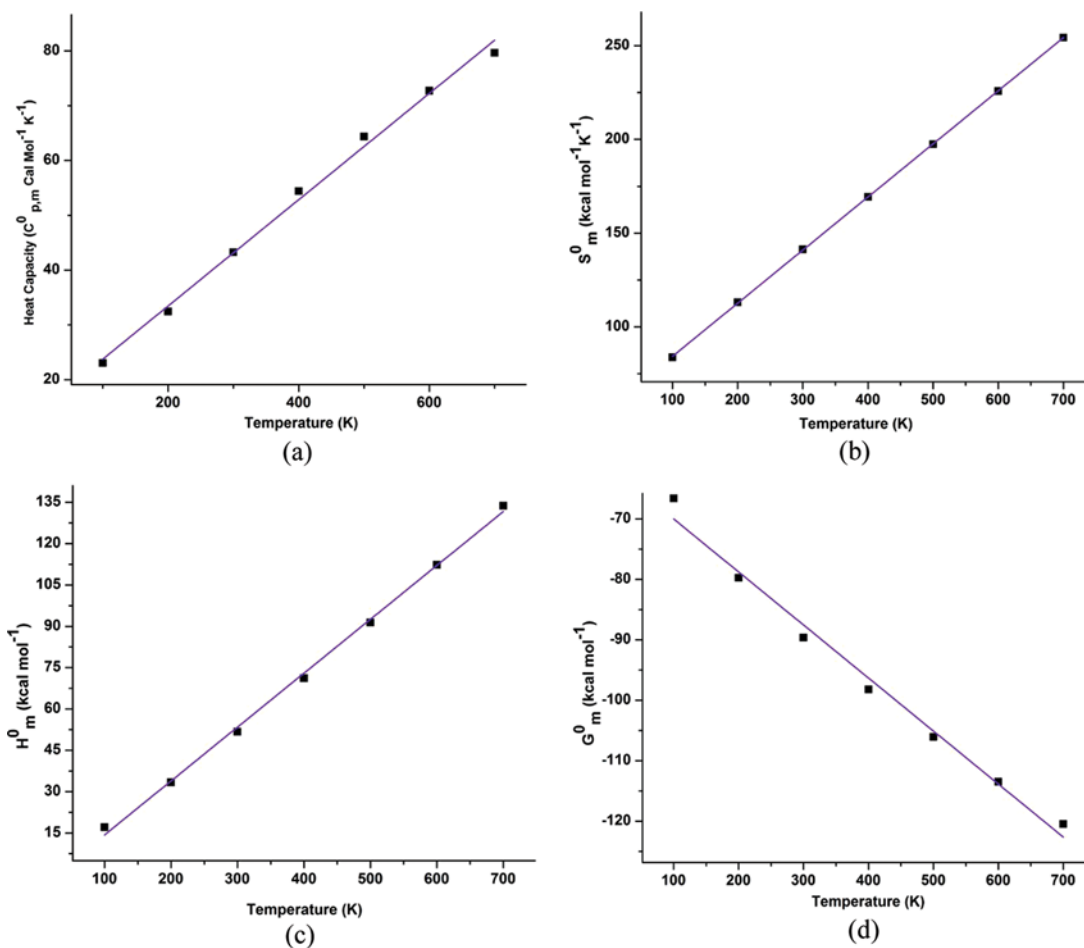
$$G_m^0 = -54.88 - 0.130T - 5.0 * 10^{-5}T^2 (R^2 = 0.998)$$

$$S_m^0 = 55.4 + 0.287T - 5.0 * 10^{-6}T^2 (R^2 = 1.000)$$

**FIGURE 9** Isodensity plots of the frontier molecular orbital of methyl L-proline hydrochloride.

**TABLE 5** Thermodynamic Properties at Different Temperatures at the B3LYP/6-311++G(d,p) Level for Methyl L-Proline Hydrochloride

T (K)	$C_{p,m}^0$ (cal mol <sup>-1</sup> K <sup>-1</sup> )	$H_m^0$ (kcal mol <sup>-1</sup> )	$G_m^0$ (kcal mol <sup>-1</sup> )	$S_m^0$ (kcal mol <sup>-1</sup> K <sup>-1</sup> )
100	23.0523	17.1012	-66.6160	83.7171
200	32.4560	33.3944	-79.7347	113.1292
300	43.2455	51.7263	-89.6414	141.3676
400	54.4163	71.1670	-98.2168	169.3839
500	64.3714	91.4112	-106.0840	197.4949
600	72.7202	112.3108	-113.4740	225.7845
700	79.6625	133.7659	-120.4840	254.2497

**FIGURE 10** Correlation graphic of various thermodynamic parameters: (a) correlation graphic of heat capacity and temperature for methyl L-proline hydrochloride; (b) correlation graphic of entropy and temperature for methyl L-proline hydrochloride; (c) correlation graphic of enthalpy and temperature for methyl L-proline hydrochloride; and (d) correlation graphic of Gibbs energy and temperature for methyl L-proline hydrochloride.

## CONCLUSION

The derivative of L-proline called methyl L-proline hydrochloride has been synthesized. The optimized geometry and IR and Raman vibrational spectra are computed for the synthesized molecule using HF and B3LYP (6-311G++(d,p)) model

chemistries. In this study, we have performed energy calculation on possible rotational isomers. Comparison between the theoretical and experimental structural parameters indicates that B3LYP is in good agreement with experimental methods. It is first time through this literature that the experimental vibrational behavior of methyl-L-proline

hydrochloride has been examined and reported along with computational insight. The energy gap and its significance between occupied and unoccupied molecular orbitals have been clearly understood. The isodensity surface contour map of the frontier orbital of HOMO and LUMO indicates the intramolecular charge transfer occurring within the molecule. After the basis of vibrational analysis of the title molecule, the thermodynamic properties of the methyl L-prolinate hydrochloride at different temperatures have been calculated, which reveals the corrections between  $C_{p,m}^0$ ,  $H_m^0$ ,  $S_m^0$ , and various temperature  $T$ .

## REFERENCES

- Kotsuki, H.; Ikishima, H.; Okuyama, A. Organocatalytic asymmetric synthesis using proline and related molecules. *Heterocycles* **2008**, *75*(4), 757–797.
- List, B. Proline catalyzed asymmetric reactions. *Tetrahedron* **2002**, *58*, 5573–5590.
- Srinivasan, M.; Perumal, S.; Selvaraj, S. (L)-Proline catalyzed efficient synthesis of 3-substituted 2,6-diarylpiperidin-4-ones. *Arkivoc* **2005**, *xi*, 201–208.
- Yang, X.; Wu, X.; Fang, M.; Yuan, Q.; Fu, E. Novel rigid chiral macrocyclic dioxopolymines derived from L-proline as chiral solvating agents for carboxylic acids. *Tetrahedron Asymm.* **2004**, *15*, 2491–2497.
- Hajos, Z. G.; Parrish, D. R. Asymmetric synthesis of bicyclic intermediates of natural product chemistry. *J. Org. Chem.* **1974**, *39*, 1615–1621.
- Roomi, M. W.; Ivanov, V.; Kalinovsky, T.; Niedzwiecki, A.; Rath, M. In vitro and in vivo antitumorigenic activity of a mixture of lysine, proline, ascorbic acid, and green tea extract on human breast cancer lines MDA-MB-231 and MCF-7. *Med. Oncol.* **2005**, *22*(2), 129–138.
- Allemann, C.; Um, J. M.; Houk, K. N. Computational investigations of the stereoselectivities of proline – related catalysts for aldol reactions. *J. Molec. Catal. A: Chem.* **2010**, *324*, 31–38.
- Wagner, C. C.; Torre, M. H.; Baran, E. J. Vibrational spectra of copper (II) complexes of L-proline. *Lat. Am. J. Pharm.* **2008**, *27*(2), 197–202.
- Mary, Y. S.; Ushakumari, L.; Harikumar, B.; Varghese, H. T.; Panicker, C. Y. FT-IR, FT-Raman and SERS spectra of L-proline. *J. Iran. Chem. Soc.* **2009**, *6*(1), 138–144.
- Li, X.-J.; Zhong, Z.-J.; Wu, H.-Z. DFT and MP2 investigations of L-proline and its hydrated complex. *J. Mol. Model* **2011**, *17*(10), 2623–2630.
- Li, J.; Sha, Y. A convenient synthesis of amino acid methyl esters. *Molecules* **2008**, *13*(5), 1111–1119.
- Frisch, M. J.; Trucks, G. W.; Schlegel, H. B.; Scuseria, G. E.; Robb, M. A.; Cheeseman, J. R.; Scalmani, G.; Barone, V.; Mennucci, B.; Petersson, G. A.; Nakatsuji, H.; Caricato, M.; Li, X.; Hratchian, H. P.; Izmaylov, A. F.; Bloino, J.; Zheng, G.; Sonnenberg, J. L.; Hada, M.; Ehara, M.; Toyota, K.; Fukuda, R.; Hasegawa, J.; Ishida, M.; Nakajima, T.; Honda, Y.; Kitao, O.; Nakai, H.; Vreven, T.; Montgomery, Jr., J. A.; Peralta, J. E.; Ogliaro, F.; Bearpark, M.; Heyd, J. J.; Brothers, E.; Kudin, K. N.; Staroverov, V. N.; Kobayashi, R.; Normand, J.; Raghavachari, K.; Rendell, A.; Burant, J. C.; Iyengar, S. S.; Tomasi, J.; Cossi, M.; Rega, N.; Millam, J. M.; Klene, M.; Knox, J. E.; Cross, J. B.; Bakken, V.; Adamo, C.; Jaramillo, J.; Gomperts, R.; Stratmann, R. E.; Yazyev, O.; Austin, A. J.; Cammi, R.; Pomelli, C.; Ochterski, J. W.; Martin, R. L.; Morokuma, K.; Zakrzewski, V. G.; Voth, G. A.; Salvador, P.; Dannenberg, J. J.; Dapprich, S.; Daniels, A. D.; Farkas, Ö.; Foresman, J. B.; Ortiz, J. V.; Cioslowski, J.; Fox, D. J. Gaussian 09, Revision A.02; Gaussian, Inc.: Wallingford, CT, 2009.
- Frisch, M. J.; Nielsm, A. B.; Holder, A. J. Gaussview User Manual; Gaussian 427: Pittsburgh, PA, 2008.
- Myung, S.; Pink, M.; Baik, M. H.; Clemmer, D. E. DL-proline. *Acta Cryst. C* **2005**, *61*, 506–508.
- Socrates, G. Infrared and Raman Characteristic Group Wave Numbers – Tables Charts, 3rd ed.; John Wiley & Sons, England, 2001.
- Roeges, N. P. G. *A Guide to the Complete Interpretation of Infrared Spectra of Organic Structures*; Wiley: New York, 1994.
- Colthup, N. B.; Daly, L. H.; Wiberly, S. E. *Introduction to Infrared and Raman Spectroscopy*; Academic Press: New York, 1975.
- Evans, J. C.; Wahr, J. C. Thermodynamic and spectroscopic study of pyrrolidine. II. Vibrational spectra and configuration. *J. Chem. Phys.* **1959**, *31*, 655.
- Gussoni, M.; Castiglioni, C. Infrared intensities. Use of the CH stretching band intensity as a tool for evaluating the acidity of hydrogen atoms in hydrocarbons. *J. Mol. Struct.* **2000**, *521*, 1–18.
- Rumi, M.; Zerbi, G. Conformational dependence of vibrational and molecular nonlinear optical properties in substituted benzenes: the role of  $\pi$ -electron conjugation and back-donation. *J. Mol. Struct.* **1999**, *509*(1), 11–28.
- Silverstein, R. M.; Webster, F. X. *Spectrometric identification of organic compounds*, 6th ed; John Wiley: Daryaganj, New Delhi, 2003.
- Rippon, W. B.; Koenig, J. L.; Walton, A. G. Raman spectroscopy of proline oligomers and poly-L-proline. *J. Am. Chem. Soc.* **1970**, *92*(25), 7455–7459.
- Smith, B. *Infrared Spectral Interpretation, A Systematic Approach*; CRC: Washington, DC, 1999.
- Mulliken, R. S. Electronic Population Analysis on LCAO -MO Molecular Wave Functions. I. *J. Chem. Phys.* **1955**, *23*, 1833–1840.
- Perepichka, D. F.; Bryce, M. R. Molecules with exceptionally small HOMO–LUMO gaps. *Angew. Chem. Int. Ed.* **2005**, *44*, 5370–5373.
- Bevan Ott, J.; Boerio-Goates, J. *Chemical Thermodynamics: Principles and Applications*; Academic Press: San Diego, CA, 2000.

Copyright of Spectroscopy Letters is the property of Taylor & Francis Ltd and its content may not be copied or emailed to multiple sites or posted to a listserv without the copyright holder's express written permission. However, users may print, download, or email articles for individual use.